DOI: 10.1002/chem.201002316

VIP

Porous Lithium Imidazolate Frameworks Constructed with Charge-Complementary Ligands

Shou-Tian Zheng,[a] Yufei Li,[a] Tao Wu,[b] Ruben A. Nieto,[a] Pingyun Feng,*[b] and Xianhui Bu*[a]

Metal–organic frameworks (MOFs) based on four-connected nodes are of special interest because of their zeolite-like topologies and open architectures.[1,2] A fundamental structural feature of zeolite topology is tetrahedral nodes (e.g., Si^{4+}) cross-linked by a bi-coordinated bridge (e.g., O^{2-} as in SiO_2). This bonding feature can be emulated by metal cations (or clusters) and organic cross-linking ligands. Until now, several metallic elements (e.g., Zn, Cd, and In) have been found to generate zeolite-like MOFs, including zeolitic imidazolate frameworks (ZIFs) and indium-based ZMOFs.[3–6] The replacement of these transition (or post-transition) metals with lightweight, main-group metals (e.g., Li, Mg, and Al) has potential to produce a lower framework density, which is desirable for enhancing gravimetric energy storage capacity of gas-storage materials. In the past several years, the synthesis of MOFs based on lightweight metals has attracted much attention with the greatest successes being achieved in Mg- and Al-MOFs.[7,8] Nevertheless, to date, the metal–organic framework based on only four-connected lithium nodes remains unknown, even though Li-containing boron imidazolate frameworks and frameworks containing Li–O clusters or chains are known.[9]

The use of Li as the framework four-connected node is very attractive because lithium is the lightest metal. However, the design and synthesis of Li-MOFs are not without significant challenges. Compared to common MOFs based on di- and trivalent metal ions, one unique feature of Li^+ is its lowest possible positive charge. For the charge balance requirement, each tetrahedral Li^+ node only needs one mono-negatively charged ligand such as imidazolate (i.e., LiL) or one-half of a dicarboxylate ligand (i.e., $LiL_{0.5}$). On the other hand, like SiO_2, four-connected MOFs require a metal/ligand ratio of 1:2, which means if imidazolate or dicarboxylate ligands are used as cross-linking ligands, the resulting 4-connected LiL_2 framework would be excessively negative (-1 per Li site for imidazolate framework or -3 for dicarboxylate framework).

In this work, we demonstrate a versatile synthetic method capable of generating a large family of Li-MOF materials. This method is based on the use of charge-complementary ligands (L^- and L^0, L = ligand) specifically chosen to mimic SiO_2 composition and to create $Li^+(L^-)(L^0)$-type Li-ZIFs. With this strategy, a total of twelve Li-ZIFs with various structures, including 2D and 3D frameworks, have been made (Table 1). As expected, two types of 3D framework materials reported here possess the general SiO_2-type framework composition of $Li^+(L^-)(L^0)$. In comparison, 2D structures contain both L^- and L^0 within the polymeric layer (i.e., $Li^+(L^-)(L^0)_{0.5}$), together with a pendant neutral ligand occupying the fourth Li^+ coordination site, leading to a general framework stoichiometry of $Li^+(L^-)(L^0)_{0.5}(L^0)$ (as in layered silicates). The three-connected lithium site with a pendant molecule in 2D structures can be desirable, because of its potential to serve as an open Li^+ site upon solvent removal. Furthermore, as shown here, pendant solvent molecules on Li sites can also serve as pillars between neutral Li/$(L^-)(L^0)$ layers to generate porosity.

Compound **1** represents the first 3D four-connected Li-ZIF. As shown in Figure 1a, each Li^+ ion in **1** is coordinated by four N atoms from two negative benzimidazolate (bim) ligands and two neutral 4,4′-bipyridine (4,4′-bpy) ligands to form a four-connected node. In turn, each organic ligand (bim and 4,4′-bpy) bridges between two Li nodes, leading to an overall 3D four-connected framework containing 1D hex-

[a] Dr. S.-T. Zheng, Y. Li, R. A. Nieto, Prof. Dr. X. Bu
Department of Chemistry and Biochemistry
California State University, Long Beach
1250 Bellflower Boulevard, Long Beach
CA 90840 (USA)
Fax: (+1) 562-985-8557
E-mail: xbu@csulb.edu

[b] T. Wu, Prof. Dr. P. Feng
Department of Chemistry
University of California, Riverside
CA 92521 (USA)
E-mail: pingyun.feng@ucr.edu

Supporting information for this article is available on the WWW under http://dx.doi.org/10.1002/chem.201002316.

Table 1. Summary of crystal data and refinement results.[a]

	Formula	Space group	a [Å]	b [Å]	c [Å]	α [°]/γ [°]	β [°]	R[F]	Net[b]
1	Li(bim)(4,4′-bpy)	$Pna2_1$	11.2007(3)	17.3036(6)	7.9293(3)	90	90	0.0412	new {6^5.8}
2	Li(im)(4,4′-bpy)	Cc	7.8645(6)	16.6945(13)	9.1195(6)	90	97.941(2)	0.0296	dia
3	Li(5,6-DMBim)(5,6-HDMBim)(4,4′-bpy)$_2$	$P\bar{1}$	10.5566(7)	18.0187(11)	18.5348(12)	83.260(5)/ 86.453(4)	74.662(4)	0.1152	0D
4	Li(bim)(bpe)$_{1/2}$·(bpe)	$P2_1/n$	9.4954(6)	10.1626(6)	22.5395(11)	90	95.911(4)	0.0566	hcb (6^3)
5	Li(bim)(pyrazine)$_{1/2}$·(CH_3CN)	$P2_1/n$	7.7706(2)	8.8075(2)	16.1226(4)	90	98.294(1)	0.0362	hcb (6^3)
6	Li(bim)(CH_3CN)$_2$	$P2_1$	7.6318(3)	9.5156(3)	8.3864(3)	90	110.474(2)	0.0333	1D
7	Li$_2$(bim)$_2$(DABCO)·(Hbim)·(CH_3CN)· DABCO·pyrazine	$P\bar{1}$	10.0374(5)	10.0674(5)	21.5782(9)	86.561(3)/ 61.901(3)	84.426(3)	0.0782	hcb (6^3)
8	[Li(bim)(dabco)$_{1/2}$·(H_2O)]$_2$·2.5 DABCO· pyrazine·CH_3CN	$Pnnm$	26.2411(6)	10.4790(3)	16.2609(4)	90	90	0.0775	hcb (6^3)
9	[Li(bim)(dabco)$_{1/2}$·(CH_3CN)]$_2$·pyrazine	$C2/c$	17.8720(2)	10.1645(11)	17.8991(2)	90	104.399(8)	0.1136	hcb (6^3)
10	[Li(bim)(pyrazine)$_{1/2}$·(4,4′-bpy)]$_2$·CH_3CN	$P2_1/n$	17.0212(3)	10.2313(2)	17.8680(3)	90	113.784(1)	0.0445	hcb (6^3)
11	Li(bim)(dabco)$_{1/2}$·(4,4′-bpy)	$Fdd2$	78.333(9)	10.3201(12)	18.1154(18)	90	90	0.0561	hcb (6^3)
12	Li(5,6-dmbim)(dabco)·CH_3CN	$Pbca$	12.1648(2)	11.8199(2)	23.5880(3)	90	90	0.0434	sq1 ($4^4.6^2$)

[a] im = imidazolate; bim = benzimidazolate; 5,6-dmbim = 5,6-dimethylbenzimidazole; 4,4′-bpy = 4,4′-bipyridine; DABCO = 1,4-diazabicyclo[2.2.2]octane; bpe = *trans*-1,2-bis(4-pyridyl)-ethylene. [b] For definitions of three-letter abbreviations, see Reticular Chemistry Structure Resource (http://rcsr.anu.edu.au/).

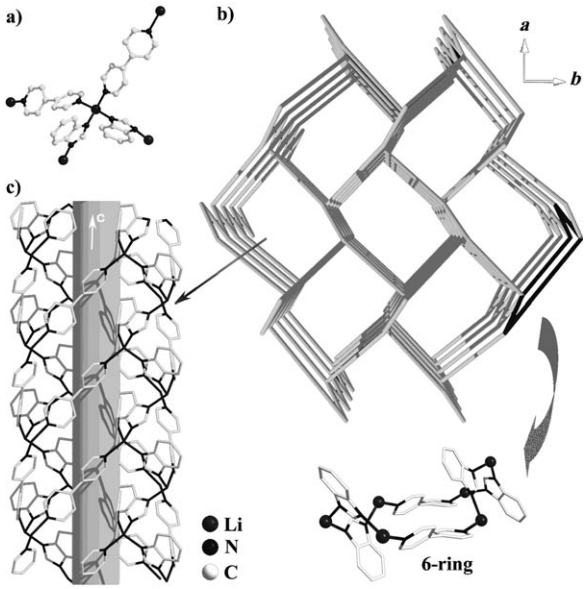

Figure 1. a) Coordination mode of Li^+ in **1**. b) View of 3D structure of **1** based on Li^+ as nodes and bim/4,4′-bpy as linker. c) View of 1D channel structure of **1**.

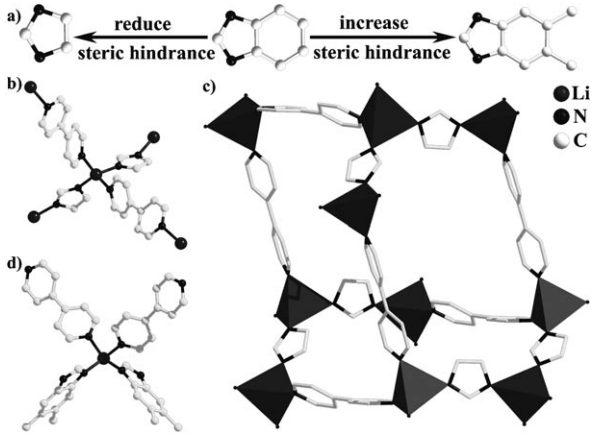

Figure 2. a) View of different negative ligands. b) and d) Coordination mode of Li^+ ions in **2** and **3**, respectively. c) View of dia structure of **2**. LiN_4 tetrahedron: grey.

agonal channels along the *c* axis (Figure 1b). The channel wall is made up of $Li_6(bim)_4(4,4'\text{-bpy})_2$ 6-rings through edge-sharing, while each channel is constructed from five infinite $[Li_6(bim)_2(4,4'\text{-bpy})_4]_\infty$ spiral chains joined together by additional bim bridges (Figure 1c, and Figure S1 in the Supporting Information). It is worth noting that the 3D framework of **1** exhibits a previously unknown four-connected uninodal topology with a vertex symbol of $6.6.6.6.6_2.10_{12}$ and a Schläfli symbol of (6^5.8).

The use of charge-complementary ligands here creates an extra freedom to tune the framework composition and topology, because either L^0 ligand or L^- ligand can be varied. The replacement of the bim ligand with imidazolate (im) or 5,6-dimethylbenzimidazolate (5,6-dmbim, Figure 2a) led to the synthesis of **2** and **3**, respectively. It is clear that substituents on the imidazolate ring have a dramatic effect on the framework structure. With the smaller im ligand, a new 3D four-connected Li-ZIF (**2**) was obtained. In the absence of any substituents on the im ring, the 3D framework of **2** exhibits an open diamond network (Figure 2b, c). However, the open pore space of the diamond net is used up by two additional diamond networks, leading to an overall threefold interpenetrated structure in **2** (Figure S2 in the Supporting Information). In comparison, the use of larger 5,6-dmbim ligand led to the formation of a discrete four-coordinated lithium complex **3**, (Figure 2d).

In addition to the use of different L^- ligands, we have also explored different neutral L^0 ligands (4,4′-bpy as shown above in **1**–**3**, *trans*-1,2-bis(4-pyridyl)-ethylene (bpe), pyrazine, and 1,4-diazabicyclo[2.2.2]octane (DABCO) described below). Compared to L^- ligands, which can be cross-linking (as in **1** and **2**) or dangling (in the form of HL and L^- as in **3**), L^0 ligands exhibit three structural roles: cross-linking,

dangling, and pore-filling. In this work, each L^0 ligand is employed individually (4,4′-bpy in **1**–**3**, bpe in **4**, pyrazine in **5**, and DABCO in **12**) or in combination with another L^0 ligand, as is the case for **7**–**11** in which two kinds of L^0 ligands (pyrazine/DABCO in **7**–**9**, pyrazine/4,4′-bpy in **10**, 4,4′-bpy/DABCO in **11**) are incorporated into structures, some as extra-framework species occupying the interlayer space (Table 1). As demonstrated below, the use of two L^0 ligands together also allows us to probe the relative bonding affinity of L^0 ligands to Li sites, which is relevant to the design of the framework materials and the creation of open Li sites. It is worth noting that the role of the L^0 ligand and the crystallization product can be altered by solvent, because solvent molecules compete for coordination to Li sites and can also be included as extra-framework species. The incorporation of solvent molecules is often desirable because it can contribute to the generation of porosity upon solvent removal.

In **4**, a longer ligand (bpe) is used, as compared to 4,4′-bpy in **1**–**3**. This results in the formation of a 2D Li-ZIF. Each tetrahedral Li center, defined by four N atoms from two L^- bim and two L^0 bpe ligands, is linked to three adjacent Li sites by two bim and one bpe ligands to form the graphite-type 2D net consisting of $Li_6(bim)_4(bpe)_2$ 6-rings (Figures 3 and 4a). The second bpe ligand on each Li site just serves as a pendant ligand (L^0-terminating) that points towards the center of the 6-ring of the adjacent layer. Such bpe ligands can be considered as a special type of pillars between two adjacent layers (Figure S3 in the Supporting Information).

In compounds **1**–**4**, L^0 ligands (4,4′-bpy and bpe) are significantly longer than L^- ligands (imidazolate-based) in terms of the distance between two N-donor sites. By using L^0 ligands (pyrazine and DABCO) with a size more comparable to that of imidazolate, additional new phases have been made. When only pyrazine is used, a new 2D Li-ZIF (**5**), also with a graphite-type net, was prepared. The layer is made of $Li_6(bim)_4(pyrazine)_2$ 6-rings (Figures 3 and 4b) with the fourth Li coordination site occupied by one pendant CH_3CN (solvent-terminating). It is of interest to note that when the concentration of pyrazine is reduced by half, pyrazine can no longer be retained as the cross-linking ligand, resulting in a 1D Li–bim chain (**6**) in which there are two pendant CH_3CN ligands at each Li site (Figure S4 in the Supporting Information). These results suggest that pyrazine is not competitive for bonding with Li and even solvent CH_3CN molecules can prevent pyrazine from bonding with Li sites.

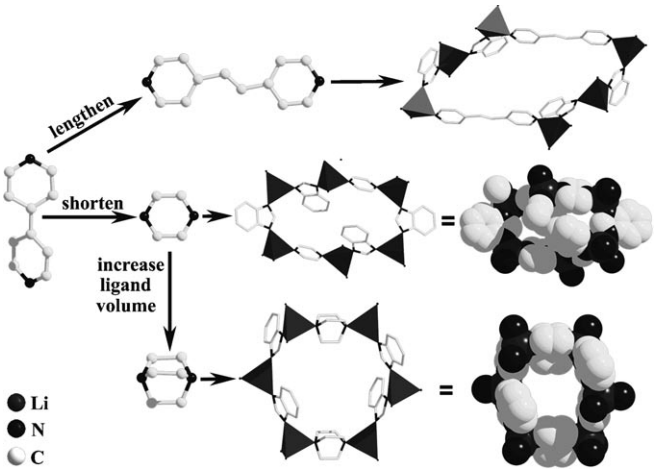

Figure 3. View of different neutral ligands and their corresponding Li_6 6-ring structures. LiN_4 tetrahedron: grey.

The use of two mixed and similar size L^0 ligands, DABCO and pyrazine (the short–short combination), led to three porous 2D Li-ZIFs (**7**–**9**; Figure S5 in the Supporting Infor-

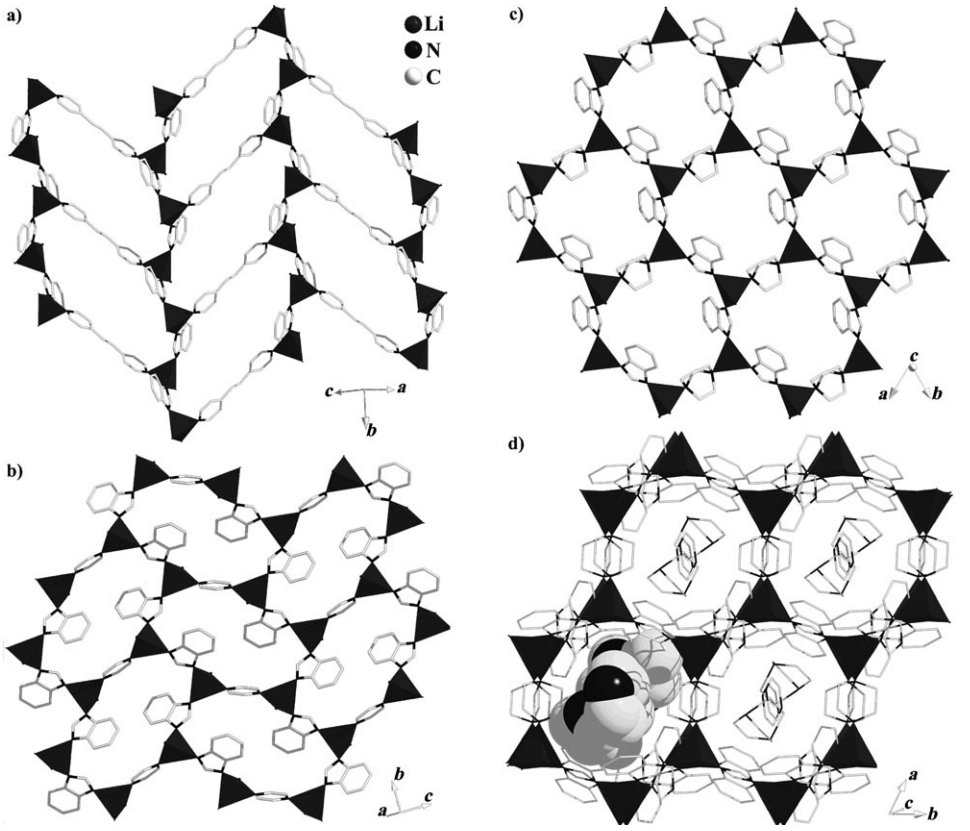

Figure 4. a)–c) View of 2D structures of **4**, **5**, and **7**, respectively. d) View of the 3D porous stacking structure of **7**. LiN_4 tetrahedron: grey.

mation) by adjusting the amount of DABCO (or pyrazine) relative to other chemicals. As shown in Figure 4c and Figure S6 (Supporting Information), the 2D layer structure of **7** consists of $Li_6(bim)_4(dabco)_2$ 6-rings with two kinds of pendant ligands, CH_3CN and Hbim alternating in the same layer (simultaneous solvent-terminating and HL-terminating). Compared with pyrazine, DABCO is more bulky. Thus, the ligands inside each $Li_6(bim)_4(dabco)_2$ 6-ring can be separated further due to increased steric hindrance. As a result, the $Li_6(bim)_4(dabco)_2$ 6-rings possess hexagonal porous rings with a diameter of $\approx$1.1 nm, while $Li_6(bim)_4(pyrazine)_2$ 6-rings in **5** are rectangular rings with the interior space occupied by bim ligands (Figure 3). The layers in **7** lie parallel to the *ab* plane and the porous $Li_6(bim)_4(dabco)_2$ 6-rings from different layers are stacked together to generate 1D infinite channels in which the uncoordinated DABCO and pyrazine are located (dual L^0-pore-filling; Figure 4d). Compounds **8** and **9** have the same polymeric Li–bim–DABCO layers as **7**, their differences lie in the types of the terminal ligands on lithium sites and extra-framework solvents molecules (pyrazine/DABCO in **7**, pyrazine/DABCO/CH_3CN in **8**, pyrazine only in **9**, Table 1). A comparison of **7**–**9** suggests that the roles of L^0 and solvent ligands and their bonding to Li sites are strongly affected by the relative concentrations of these species (in addition to their chemical structures). All these variations provide multiple ways to pillar the 2D layers and to fill the interlayer pore space for porosity control.

In addition to DABCO/pyrazine used for **7**–**9**, the use of mixed size-complementary DABCO/4,4′-bpy or pyrazine/4,4′-bpy (the long–short combination), led to 2D Li-ZIFs **10** and **11**. The common feature in **10** and **11** is that short neutral ligands (DABCO or pyrazine) serve as cross-linkers in the construction of hexagonal $Li_6(bim)_4(dabco)_2$ or $Li_6(bim)_4(pyrazine)_2$ 6-rings, respectively, while long neutral ligands 4,4′-bpy serve as pendant ligands (Figure S7 in the Supporting Information). Combining all above results, it is proposed here that the tendency of L^0 ligands to serve as cross-linking ligands follows the order: DABCO > pyrazine > 4,4′-bpy. The tendency to serve as dangling ligands is 4,4′-bpy > CH_3CN > pyrazine > DABCO (no pendant DABCO has been observed so far). Furthermore, with the exception of long 4,4′-bpy and bpe ligands, short DABCO, pyrazine, and CH_3CN have also been found to serve as the pore-filling molecules.

The formation of the graphite-type topology in compounds **4** and **5** and **7**–**11** highlights a unique ability to create "pillared" Li-ZIF structures with pores controlled by L^0 and solvent molecules. This is in part due to the different bonding strength between Li–L^- and Li–L^0. Furthermore, the relative strength between the lithium–ligand bond and ligand–ligand steric repulsion also plays a role. In Zn-based ZIFs, the ligand–ligand steric repulsion is not strong enough to prevent the formation of im-Zn-im linkages, even though it is strong enough to change the 3D topological types. In comparison, in the Li-ZIF system, the ligand–ligand repulsion also contributes to the formation of low-dimensional structures, because of relatively weaker Li–L^0 bond. On the basis of this work, it can be suggested that in the Li-ZIF system, longer cross-linking ligands (e.g., 4,4′-bpy) may have a stronger tendency to form 3D structures through reduced ligand–ligand repulsion, while a shorter cross-linking ligand (e.g., DABCO) may adopt lower dimensional structures to better relieve the steric repulsion. Thus, both 3D and 2D frameworks are accessible through the ligand choice. One interesting aspect of this work is that even with the same 2D net topology, there are great variations in these structures as evidenced by the differences in 1) the cross-linking L^0 ligand, 2) pendant pillaring ligands, and 3) the pore-filling L^0 ligands or solvent molecules. These differences can significantly alter their porous properties.

All aforementioned DABCO-containing Li-ZIFs were made with bim. Because it was observed here (see below) that DABCO-containing compounds tend to give materials with a large solvent accessible volume, we further studied the effect of replacing bim with the larger 5,6-dmbim ligand in the DABCO system, which led to a new 2D Li-ZIF **12** built from square-shaped 4-rings $Li_4(5,6\text{-dmbim})_2(dabco)_2$ with a chessboard-like pattern (Figure 5). The dimensions of the Li_4 4-ring are 0.59×0.71 nm, which is smaller than that of Li_6 6-ring. The layers are parallel to the *ab* plane and stacked together to form 1D channels along the *c* axis, in which CH_3CN molecules are located (Figure S8 in the Supporting Information).

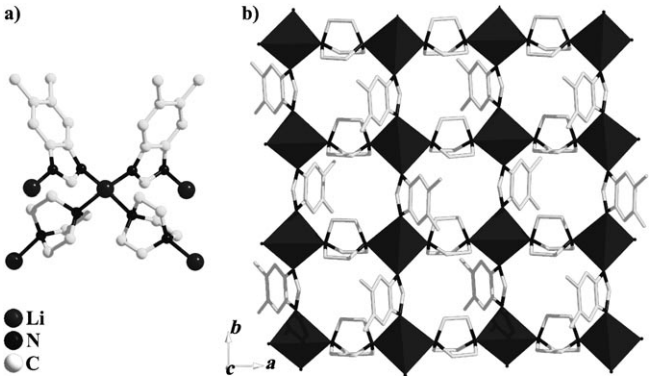

Figure 5. a) Coordination mode of Li^+ ion in **12**. b) View of the 2D structure of **12**. LiN_4 tetrahedron: grey.

The total potential solvent accessible volumes calculated with PLATON,[10] are 8.5 (for **1**), 33.2 (for **7**), 60.4 (for **8**), 27.1 (for **9**) and 20.0% (for **12**), which correlate well with the ratio (0, 1, 2.25, 0.5, and 1, respectively) between the number of uncoordinated solvent molecules and the number of Li sites. One anomaly from this trend is compound **12**, which can be explained by its two methyl groups on the cross-linking ligand (5,6-dmmim) that block the pores and smaller pore-filling solvent molecules (CH_3CN). To determine porous properties of such materials, products **1**, **7**, and **8** were selected for gas-adsorption measurements performed on a Micromeritics ASAP 2010 surface-area and pore-size analyzer. These samples were degassed at room temperature

for 24 h under vacuum prior to the measurement. The maximum CO_2 adsorptions of **1**, **7**, and **8** at 273 K and 1 atm are 9.1, 27.8 and 48.8 $cm^3 g^{-1}$, respectively (Figure 6), which

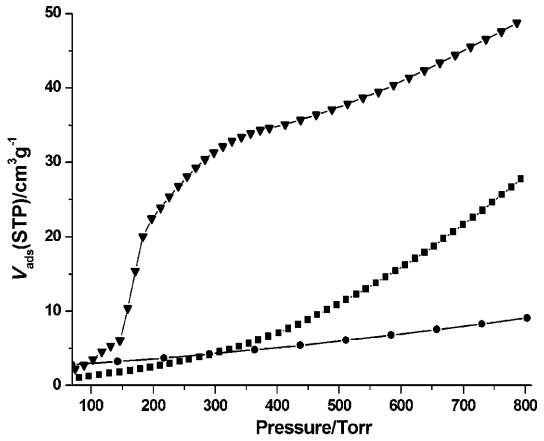

Figure 6. CO_2 adsorption isotherms of **1** (●), **7** (■), and **8** (▲) at 273 K.

agree well with the trend in the calculated solvent accessible volumes in these phases (8.5, 33.2, and 60.4%, respectively). The CO_2 uptake in **8** is very high and is in fact higher than the CO_2 uptake (35.6 $cm^3 g$) by BIF-9-Li, which is a porous Li-B imidazolate framework with zeolite RHO-type topology.[9d] Additionally, the CO_2 storage capacities of some highly porous ZIFs are in the range of 19–55 $cm^3 g^{-1}$ under the same conditions.[1b] However, likely due to the limitation of pore aperture, **1**,**7**, and **8** do not show appreciable N_2 adsorption.

In summary, a family of lithium imidazolate frameworks has been synthesized by using the charge-complementary-ligand strategy, which is designed to control the local charge density surrounding the lithium sites and to allow the formation of SiO_2-like structure that have so far been rather rare for Li-ZIFs. These lithium imidazolate frameworks, mediated with neutral ligands, not only exhibit various types of structures, but also tunable porous features and gas sorption properties. Such results reported here demonstrate that the charge-complementary-ligand synthetic strategy is an effective synthetic method for generating interesting Li-based porous materials with potential applications in gas sorption.

Experimental Section

Typical synthesis of 1: Li_2S (0.092 g, 2 mmol), bim (0.110 g, 1 mmol), 4,4′-bpy (0.156 g, 1 mmol), and CH_3CN (3.0 g) were placed in a 20 mL vial. The sample was heated at 90 °C for 5 days, and then cooled to room-temperature. After washed by acetone, the colorless crystals were obtained.

Synthesis of 2–12: Compounds **2** and **3** were prepared in a similar manner to **1**, except for the replacement of bim by im (0.062 g, 1 mmol) and 5,6-dmbim (0.069 g, 0.5 mmol), respectively. Compounds **4** and **6–11** were prepared in a similar manner to **1**, except for the replacement of 4,4′-bpy by bpe (0.182 g, 1.0 mmol), pyrazine (0.080 g, 1 mmol), DABCO·6H_2O/pyrazine (0.110 g, 0.5 mmol/0.156 g, 2.0 mmol), DABCO·6H_2O/pyrazine (0.220 g, 1.0 mmol/0.156 g, 2.0 mmol), DABCO·6H_2O/pyrazine (0.110 g, 0.5 mmol/0.078 g, 1.0 mmol), pyrazine/4,4′-bpy (0.156 g, 1.43 mmol/0.156 g, 1.0 mmol), and 4,4′-bpy/DABCO·6H_2O (0.156 g, 1.0 mmol/0.110 g, 0.5 mmol), respectively. Compound **5** was prepared in a similar manner to **6**, except for the replacement of bim/pyrazine (0.110 g, 1.0 mmol/0.08 g, 1.0 mmol) by bim/pyrazine (0.055 g, 0.50 mmol/0.156 g, 1.0 mmol). Compound **12** was prepared in a similar manner to **3**, except for the replacement of 4,4′-bpy by DABCO·6H_2O (0.165 g, 0.75 mmol).

Crystal structure determination: Each crystal was glued to a glass fiber with epoxy resin and mounted on a Bruker APEX II diffractometer equipped with a fine focus, 2.0 kW sealed-tube X-ray source ($Mo_{K\alpha}$ radiation, $\lambda = 0.71073$ Å) operating at 50 kV and 30 mA. The empirical absorption correction was based on equivalent reflections. Each structure was solved by direct methods followed by successive difference Fourier methods. All non-hydrogen atoms were refined anisotropically. Computations were performed using SHELXTL[11] and final full-matrix refinements were against F^2. CCDC-777431 (**1**), -777432 (**2**), -777433 (**3**), -777434 (**4**), -777435 (**5**), -777436 (**6**), -777437 (**7**), -777438 (**8**), -777439 (**9**), -777440 (**10**), -777441 (**11**) and -777442 (**12**) contain the supplementary crystallographic data for this paper. These data can be obtained free of charge from The Cambridge Crystallographic Data Centre via www.ccdc.cam.ac.uk/data_request/cif.

Other physical measurements: Gas adsorption measurements (H_2, CO_2, and N_2) were performed on a Micromeritics ASAP 2020 surface-area and pore-size analyzer. Thermal analyses were performed in a dynamic nitrogen atmosphere with a heating rate of 10 °C min^{-1}, using a SDTQ600 thermal analyzer. Powder XRD patterns were obtained using a Bruker D8 Avance X-ray powder diffractometer with $Cu_{K\alpha}$ radiation ($\lambda =$ 1.54056 Å).

Acknowledgements

We thank the support of this work by NSF (X.B. DMR-0846958, P.F. CHEM-0809335), Research Corporation (X.B. CC6593), and DOE (P.F. DE-SC0002235), and. X.B is a Henry Dreyfus Teacher Scholar.

Keywords: lithium · metal–organic frameworks · mesoporous materials

[1] a) G. Férey, *Chem. Soc. Rev.* **2008**, *37*, 191; b) A. Phan, C. J. Doonan, F. J. Uriberomo, C. B. Knobler, M. O'Keefee, O. M. Yaghi, *Acc. Chem. Res.* **2010**, *43*, 58.

[2] a) R. E. Morris, P. S. Wheatley, *Angew. Chem.* **2008**, *120*, 5044; *Angew. Chem. Int. Ed.* **2008**, *47*, 4966; b) K. Koh, A. G. Wong-Foy, A. J. Matzger, *J. Am. Chem. Soc.* **2009**, *131*, 4184.

[3] a) H. Hayashi, A. P. Côté, H. Furukawa, M. O'Keeffe, O. M. Yaghi, *Nat. Mater.* **2007**, *6*, 501; b) R. Banerjee, A. Phan, B. Wang, C. Knobler, H. Furukawa, M. O'Keeffe, O. M. Yaghi, *Science* **2008**, *319*, 939–943; c) L. Pan, D. H. Olson, L. R. Ciemnolonski, R. Heddy, J. Li, *Angew. Chem.* **2006**, *118*, 632; *Angew. Chem. Int. Ed.* **2006**, *45*, 616; d) K. Li, D. H. Olson, J. Seidel, T. J. Emge, H. Gong, H. Zeng, J. Li, *J. Am. Chem. Soc.* **2009**, *131*, 10368; e) J. An, R. P. Fiorella, S. J. Geib, N. L. Rosi, *J. Am. Chem. Soc.* **2009**, *131*, 8401; f) T. T. Luo, H. C. Wu, Y. C. Jao, S. M. Huang, T. W. Tseng, Y. S. Wen, G. H. Lee, S. M. Peng, K. L. Lu, *Angew. Chem.* **2009**, *121*, 9625; *Angew. Chem. Int. Ed.* **2009**, *48*, 9461; g) J. An, S. J. Geib, N. L. Rosi, *J. Am. Chem. Soc.* **2010**, *132*, 38.

[4] a) X. H. Bu, M. L. Tong, H. C. Chang, S. Kitagawa, S. R. Batten, *Angew. Chem.* **2004**, *116*, 194; *Angew. Chem. Int. Ed.* **2004**, *43*, 192; b) B. Chen, N. W. Ockwig, A. R. Millward, D. S. Contreras, O. M. Yaghi, *Angew. Chem.* **2005**, *117*, 4823; *Angew. Chem. Int. Ed.* **2005**, *44*, 4745; c) X. C. Huang, Y. Y. Lin, J. P. Zhang, X. M. Chen, *Angew. Chem.* **2006**, *118*, 1587; *Angew. Chem, Int. Ed.* **2006**, *45*, 1557;

d) L. J. Murray, M. Dincă, J. R. Long, *Chem. Soc. Rev.* **2009**, *38*, 1294; e) Y. Yan, I. Telepeni, S. Yang, X. Lin, W. Kockelmann, A. Dailly, A. J. Blake, W. Lewis, G. S. Walker, D. R. Allan, S. A. Barnett, N. R. Champness, M. Schröder, *J. Am. Chem. Soc.* **2010**, *132*, 4092; f) S. Xiang, W. Zhou, J. M. Gallegos, Y. Liu, B. Chen, *J. Am. Chem. Soc.* **2009**, *131*, 12415; g) Y. Q. Tian, S. Y. Yao, D. Gu, K. H. Cui, D. W. Guo, G. Zhang, Z. X. Chen, D. Y. Zhao, *Chem. Eur. J.* **2010**, *16*, 1137.

[5] a) L. Ma, W. Lin, *Angew. Chem.* **2009**, *121*, 3691; *Angew. Chem. Int. Ed.* **2009**, *48*, 3637; b) L. Ma, A. Jin, Z. Xie, W. Lin, *Angew. Chem.* **2009**, *121*, 10089; *Angew. Chem. Int. Ed.* **2009**, *48*, 9905; c) M. Tonigold, Y. Lu, B. Bredenkötter, B. Rieger, S. Bahnmüller, J. Hitzbleck, G. Langstein, D. Volkmer, *Angew. Chem.* **2009**, *121*, 7682; *Angew. Chem. Int. Ed.* **2009**, *48*, 7546; d) D. Zhao, D. Yuan, D. Sun, H. C. Zhou, *J. Am. Chem. Soc.* **2009**, *131*, 9186; e) B. Xiao, P. J. Byrne, P. S. Wheatley, D. S. Wragg , X. Zhao, A. J. Fletcher, K. M. Thomas, L. Peters, J. S. O. Evans, J. E. Warren, W. Zhou, R. E. Morris, *Nat. Chem.* **2009**, *1*, 289; f) J. R. Li, D. J. Timmons, H. C. Zhou, *J. Am. Chem. Soc.* **2009**, *131*, 6368; g) M. B. Duriska, S. M. Neville, J. Lu, S. S. Iremonger, J. F. Boas, C. J. Kepert, S. R. Batten, *Angew. Chem.* **2009**, *121*, 9081; *Angew. Chem. Int. Ed.* **2009**, *48*, 8919.

[6] a) J. Y. Sun, L. H. Weng, Y. M. Zhou, J. X. Chen, Z. X. Chen, Z. C. Liu, D. Y. Zhao, *Angew. Chem.* **2002**, *114*, 4651; *Angew. Chem. Int. Ed.* **2002**, *41*, 4471; b) Z. Lin, A. M. Z. Slawin, R. E. Morris, *J. Am. Chem. Soc.* **2007**, *129*, 4880; c) D. F. Sava, V. C. Kravtsov, J. Eckert, J. F. Eubank, F. Nouar, M. Eddaoudi, *J. Am. Chem. Soc.* **2009**, *131*, 10394; d) F. Nouar, J. Eckert, J. F. Eubank, P. Forster, M. Eddaoudi, *J. Am. Chem. Soc.* **2009**, *131*, 2864; e) S. Huh, T. H. Kwon, N. Park, S. J. Kimc, Y. Kim, *Chem. Commun.* **2009**, 4953; f) K. C. Stylianou, R. Heck, S. Y. Chong, J. Bacsa, J. T. A. Jones, Y. Z. Khimyak, D. Bradshaw, M. J. Rosseinsky, *J. Am. Chem. Soc.* **2010**, *132*, 4119.

[7] a) T. Loiseau, L. Lecroq, C. Volkrnger, J. Marrot, G. Férey, M. Haouas, F. Taulelle, S. Bourrelly, P. L. Llewellyn, M. Latroche, *J. Am. Chem. Soc.* **2006**, *128*, 10223; b) A. Comotti, S. Bracco, P. Sozzani, S. Horike, R. Matsuda, J. Chen, M. Takata, Y. Kubota, S. Kitagawa, *J. Am. Chem. Soc.* **2008**, *130*, 13664; c) Y. E. Cheon, J. Park, M. P. Suh, *Chem. Commun.* **2009**, 5436; d) T. Ahnfeldt, N. Guillou, D. Gunzelmann, I. Margiolaki, T. Loiseau, G. Férey, J. Senker, N. Stock, *Angew. Chem.* **2009**, *121*, 5265; *Angew. Chem. Int. Ed.* **2009**, *48*, 5163.

[8] K. Sumida, M. R. Hill, S. Horike, A. Dailly, J. R. Long, *J. Am. Chem. Soc.* **2009**, *131*, 15120.

[9] a) D. J. MacDougall, J. J. Morris, B. C. Noll, K. W. Henderson, *Chem. Commun.* **2005**, 456; b) D. Banerjee, L. A. Borkowski, S. J. Kim, J. B. Parise, *Cryst. Growth. Des.* **2009**, *9*, 4922; c) J. Zhang, T. Wu, C. Zhou, S. Chen, P. Feng, X. Bu, *Angew. Chem.* **2009**, *121*, 2580; *Angew. Chem. Int. Ed.* **2009**, *48*, 2542; d) T. Wu, J. Zhang, C. Zhou, L. Wang, X. Bu, P. Feng, *J. Am. Chem. Soc.* **2009**, *131*, 6111; e) B. F. Abrahams, M. J. Grannas, T. A. Hudson, R. Robson, *Angew. Chem.* **2010**, *122*, 1105; *Angew. Chem. Int. Ed.* **2010**, *49*, 1087.

[10] PLATON, A Multipurpose Crystallographic Tool, A. L. Spek, Utrecht University, Utrecht (The Netherlands), **2003**.

[11] G. M. Sheldrick, *Acta Cryst.* **2008**, *A64*, 112-122.

Received: August 13, 2010
Published online: October 28, 2010

